

Article

A Novel Viscosity-Temperature Model of Glass-Forming Liquids by Modifying the Eyring Viscosity Equation

Chunyu Chen ¹, Huidan Zeng ^{1,*}, Yifan Deng ¹, Jingtao Yan ¹, Yeja Jiang ¹, Guorong Chen ¹, Qun Zu ^{2,*} and Luyi Sun ³

¹ Key Laboratory for Ultrafine Materials of Ministry of Education, School of Materials Science and Engineering, East China University of Science and Technology, Shanghai 200237, China;

Y30180377@mail.ecust.edu.cn (C.C.); Y30160394@mail.ecust.edu.cn (Y.D.);

Y45180095@mail.ecust.edu.cn (J.Y.); Y45160041@mail.ecust.edu.cn (Y.J.); grchen@ecust.edu.cn (G.C.)

² Nanjing Glass Fiber Research and Design Institute, Sinoma Science and Technology Co., Ltd., Nanjing 210012, China

³ Polymer Program, Institute of Materials Science and Department of Chemical & Biomolecular Engineering, University of Connecticut, Storrs, CT 06269, USA; luyi.sun@uconn.com

* Correspondence: hdzeng@ecust.edu.cn (H.Z.); zuqun@fiberglasschina.com (Q.Z.)

Received: 19 October 2019; Accepted: 2 January 2020; Published: 7 January 2020



Abstract: Many models have been created and attempted to describe the temperature-dependent viscosity of glass-forming liquids, which is the foundational feature to lay out the mechanism of obtaining desired glass properties. Most viscosity models were generated along with several impact factors. The complex compositions of commercial glasses raise challenges to settle these parameters. Usually, this issue will lead to unsatisfactory predicted results when fitted to a real viscosity profile. In fact, the introduction of the reliable viscosity-temperature data to viscosity equations is an effective approach to obtain the accurate parameters. In this paper, the Eyring viscosity equation, which is widely adopted for molecular and polymer liquids, was applied in this case to calculate the viscosity of glass materials. On the basis of the linear variation of molar volume with temperature during glass cooling, a modified temperature-dependent Eyring viscosity equation was derived with a distinguished mathematical expression. By means of combining high-temperature viscosity data and the glass transition temperature (T_g), nonlinear regression analysis was employed to obtain the accurate parameters of the equation. In addition, we have demonstrated that the different regression methods exert a great effect on the final prediction results. The viscosity of a series of glasses across a wide temperature range was accurately predicted via the optimal regression method, which was further used to verify the reliability of the modified Eyring equation.

Keywords: viscosity model; glass; Eyring equation; glass transition temperature

1. Introduction

Viscosity is of great significance for the processing of glasses or glass-ceramics due to its decisive role in the steps of melting, pressing, forming, and annealing [1]. However, the temperature-dependent viscosity changes cannot be measured in glass with a single experimental technique, since the viscosity varies during melting to formation [2,3]. Moreover, the high cost of measuring glass viscosity and the difficulty of measuring the range of low viscosity, restrict its real practice. To accurately fit the viscosity-temperature curve, researchers have taken great efforts to manage glass viscosity, through controlling each correlated contributor such as temperature [4,5], compositions [6,7], structure [8,9], thermal history [10,11], etc.

Over the past few years, the analysis of experimental data has contributed to the modeling of temperature-dependent viscosity. The classical Vogel-Fulcher-Tammann (VFT) equation [12,13], a three-parameter model that works well for glasses with variable compositions, is suitable to predict viscosity across more than 10 orders of magnitude. The VFT equation was proposed mathematically based on the analysis of viscosity and widely applied in the glass company. Following the VFT equation, other three-parameter models were later developed, such as the Adam–Gibbs equation (AG) [14], the Avramov–Milchev (AM) equation [15], and the Mauro–Yue–Ellison–Gupta–Allan (MYGEA) equation [16]. The AM model was developed on the assumption of random probability distribution of activation energies for molecular transport due to structural disorder. MYGEA was derived from the analysis of energy landscape and the temperature-dependent constraint theory for configuration entropy. Generally speaking, if the viscosity of glass-forming liquids is low enough, it would result in a linear relationship between $\ln \eta$ and $1/T$ so that the modeling is relatively simple. However, it remains a great challenge for the phenomenon of overfitting when it comes to the high-viscosity region [17]. Therefore, it is highly desirable to predict the viscosity more accurately by constructing an improved model using different mathematical expressions.

Liquid viscosity is also one of the most important properties of chemical transportation, thus many viscosity models of molecular and polymer liquids have been developed in this area. Among them, glass-forming liquids belong to the Newtonian fluids, which are in category of many other similar organic or inorganic liquids [2,18,19] and have been extensively studied. The Arrhenius equation was firstly used for the viscosity calculation of fluids many years ago, i.e., $\ln \eta = A + B/T$, where A and B are dependent of composition, with T being the temperature. However, the Arrhenius equation is habitually suitable for the low-viscosity range [20], which means non-Arrhenius behavior would occur when the temperature drops because the changes of network structures become the main factors that influence the viscosity [20]. The Eyring viscosity equation as a conventional method was derived from Eyring's absolute rate theory, which is used to define the viscous flow of a liquid as the activation process [21]. Thus far, many modified models have been established by improving the calculation accuracy of activation energy in the Eyring equation. Among these studies, a model with connectivity of the activation volume to the activation energy was used for fitting the pressure-dependent viscosity of liquids at a constant temperature, and the calculated values were in good agreement with the measured results [22–25]. However, the properties of glass in the forming process is hardly influenced by pressure, so the impact of pressure can be neglected [26]. Through this theory, denoting the temperature-dependent parameters in the model as specific expressions is a feasible way to study the viscosity-temperature relationship of the glass-forming liquids.

The viscosity-temperature model based on the Eyring pressure equation was constructed for viscosity and basic thermodynamic features of glass-forming liquids. Through the calculation, it was found that the modified Eyring viscosity equation showed accuracy of fit to the experimental data in the entire temperature range, especially at low-temperature region, which overcame the previous limitations and broadened its potential applications.

2. Modeling

According to Eyring's absolute rate theory, the viscosity of a liquid is given by [27,28]:

$$\eta = \frac{hN_A}{V_m} \exp\left(\frac{E_0}{RT}\right) \quad (1)$$

where η , h , N_A , V_m , E_0 , and R are the dynamic viscosity, Planck's constant, Avogadro's number, molar volume of the liquid, activation free energy for viscous flow, and the ideal gas constant, respectively.

To describe the pressure dependence of viscosity, the volume of activation was introduced as follows [29,30]:

$$\eta = A \exp\left(\frac{pV_0}{RT}\right). \quad (2)$$

where A is a prefactor, which is dependent on temperature, p is pressure, and V_0 is the volume of activation. Parameter A should be expressed as a function of temperature to describe the temperature dependence of glass viscosity. Combining Equations (1) and (2), the Eyring model can be expressed as follows, in which, the similar form can be found in the literature [31]:

$$\eta = \frac{B}{V_m} \exp\left(\frac{pV_0}{RT}\right) \quad (3)$$

where B is a prefactor that is independent of temperature. The volume of activation is often considered as a constant [24]. However, it is dependent on pressure and temperature. Due to having little practical consequence for glass-forming or glass-processing, pressure is not taken into account [32], so V_0 can be described as [22]:

$$V_0 = k(T)V_m \quad (4)$$

where k is the ratio of the activation volume to molar volume and the function of temperature. This ratio should be equal to that ratio of the number of activated particles to the total number of particles—that is, the probability of the occurrence of an activated particle. According to the Boltzmann distribution law, k can be given by:

$$k(T) = \alpha e^{-\frac{\beta}{T}} \quad (5)$$

where α and β are composition-dependent constants. The change in volume during glass forming is shown in Figure 1. Above T_g , the molar volume (V_m) changes almost linearly with temperature. The crossover of the nonequilibrium state (at low temperatures) and the linear expansion of the equilibrium state (at high temperatures) allow the T_g values to be determined, which has been confirmed by both experiments and simulations [33–36]. Despite a sudden change in the slope of V_m versus T in the glass transition region, it does not often have a significant effect on the relationship between viscosity and temperature, because the casting temperature is above T_g . If the mass of glass remains constant, we can assume when $T > T_g$, molar volume is an appropriate linear function of temperature:

$$V_m = aT + b \quad (6)$$

where a and b are related to glass compositions.

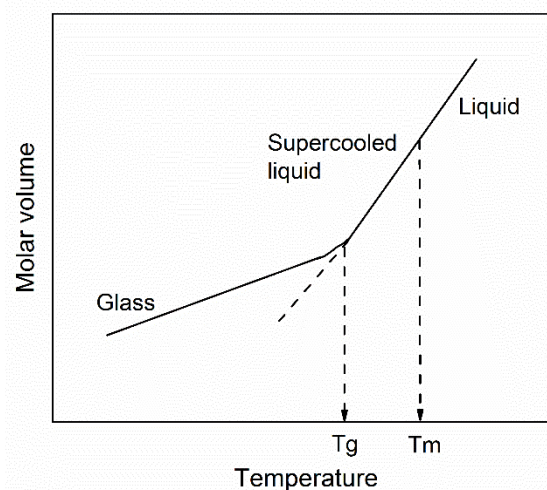


Figure 1. Schematic representation of molar volume as a function of the temperature of a glass liquid [37].

Putting Equations (4)–(6) into (3), the following Equation (7) is obtained:

$$\eta = \frac{B}{aT + b} \exp\left(\frac{p\alpha e - \frac{\beta}{T}}{RT}(aT + b)\right) \quad (7)$$

Equation (7) becomes:

$$\eta = \frac{1}{CT + D} \exp\left(\frac{He - \frac{\beta}{T}}{RT}(CT + D)\right) \ln \eta = \ln \frac{1}{CT + D} + \frac{He - \frac{\beta}{T}}{RT}(CT + D) \quad (8)$$

where $C = a/B$, $D = b/B$, and $H = Bp\alpha$. C , D , H , and β are regressed by experimental data.

3. Calculation

The new model of Equation (8) was used to correlate the dynamic viscosity of glasses, from T_g to higher temperatures. Because the viscosity in the high-temperature region is more easily measured than the viscosity at the low-temperature region, the experimental viscosity data at high temperatures can be fitted to Equation (8), and C , D , H , and β are obtained. Then, the model is extrapolated to predict the low-temperature viscosity. The nonlinear regression method was employed and implemented by using MATLAB. An example of a calculation is given by fitting Equation (8) to the viscosity data of 7.9Cs₂O-23.2CaO-66.7SiO₂-1Fe₂O₃ (mol%) from the literature [38]. The corresponding data are plotted in Figure 2a, where the data in the red circle came from fitting results.

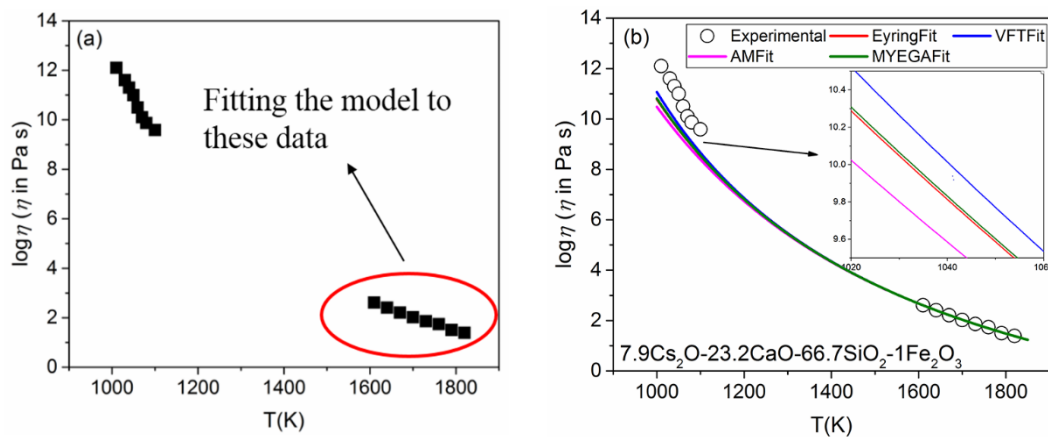


Figure 2. (a) Viscosity data of 7.9Cs₂O-23.2CaO-66.7SiO₂-1Fe₂O₃ (the data in the red circle are for fitting); (b) results of the low-temperature extrapolation of the four models.

The same regression method was also applied in three other classic models—VFT, AM, and MYEGA—and their predictions were compared in the low-temperature range. Three expressions are written in terms of fragility [16]:

VFT:

$$\log_{10} \eta(T) = \log_{10} \eta_{\infty} + \frac{(12 - \log_{10} \eta_{\infty})^2}{m\left(\frac{T}{T_g} - 1\right) + (12 - \log_{10} \eta_{\infty})} \quad (9)$$

AM:

$$\log_{10} \eta(T) = \log_{10} \eta_{\infty} + (12 - \log_{10} \eta_{\infty}) \left(\frac{T_g}{T}\right)^{m/(12 - \log_{10} \eta_{\infty})} \quad (10)$$

MYEGA:

$$\log_{10} \eta(T) = \log_{10} \eta_{\infty} + (12 - \log_{10} \eta_{\infty}) \frac{T_g}{T} \exp \left[\left(\frac{m}{12 - \log_{10} \eta_{\infty}} - 1 \right) \left(\frac{T_g}{T} - 1 \right) \right] \quad (11)$$

where η_{∞} is infinite temperature viscosity and m is fragility. The parameters are listed in Table 1. Figure 2b illustrates temperature dependence of the viscosity of 7.9Cs₂O-23.2CaO-66.7SiO₂-1Fe₂O₃. According to the previous research, the VFT model always overpredicts the values of viscosity at low temperatures [13,39], especially for the liquids with high fragility [16]. Clearly, none of the results predicted at a low-temperature (1010 to 1100 K) extrapolation of the four models is close to the experimental data. It shows that the fitting method has a direct impact on the final prediction.

Table 1. Obtained parameters of 7.9Cs₂O-23.2CaO-66.7SiO₂-1Fe₂O₃ in the modified Eyring model.

Parameters	$\log \eta_{\infty}$	m	T_g (K)	—
VFT	−5.63	30.35	968.57	—
AM	−4.2	26.14	940.99	—
MYEGA	−5.39	28.42	957.34	—
Parameters	C	D	H	β
Eyring	−5.02	62258.58	2.92	−578.54

How to accurately estimate the $\log \eta$ versus T function at low temperatures is a tough problem. The most widely accepted definition of T_g is raised by Angell, who defined T_g as the corresponding temperature when the value of viscosity is equal to 10¹² Pa·s [40]. T_g can be measured by simple thermal analysis. Therefore, we treat the points as fitting data as shown in Figure 3a. The predicted results are significantly improved, especially the predicted values of high-viscosity, are in good agreement with the experimental results. Coefficients of determination (R^2) listed in Table 2 are all over 0.999. Meanwhile, it is found that the obtained $\log \eta_{\infty}$ and m from different models by the same fitting method also have a certain difference, especially $\log \eta_{\infty}$. It shows that more errors occur when using different models of the same parameter. Viscosity is often affected by many factors that impact obvious limitations on viscosity modeling, such as thermal history, composition, etc.

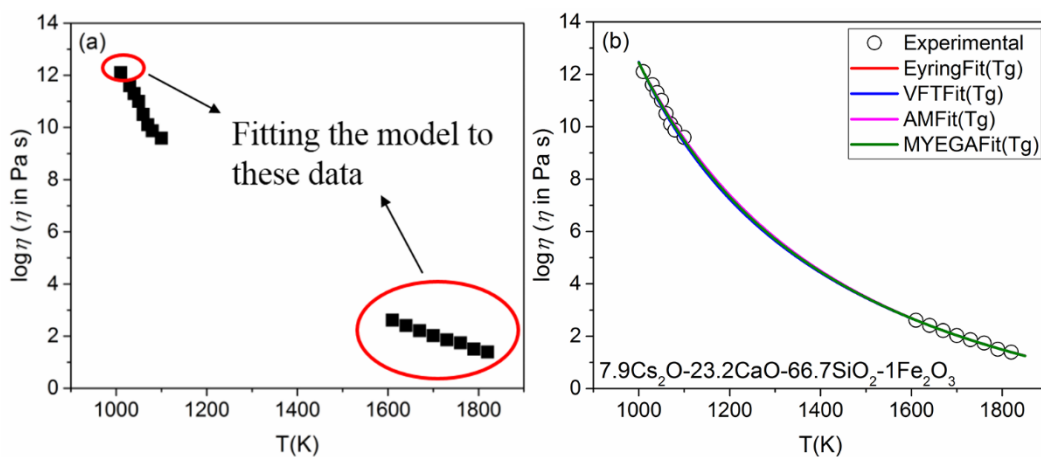


Figure 3. (a) Viscosity data of 7.9Cs₂O-23.2CaO-66.7SiO₂-1Fe₂O₃ (the data in the red circle are for fitting); (b) results of the low-temperature extrapolation test of the four models.

Note that this study does not focus on comparing the physical significance of these models. Following this work, the viscosity data of other glass compositions are further validated through this modified Eyring model. The viscosity data of different glasses were collected, including borate [41],

silicate [42], borosilicate glasses [43], anorthite and diopside [28], chalcogenide system Se-Te [44], and metallic liquid [45]. The calculated data are shown in Figure 4 with a good fit to viscosity-temperature data of these amorphous materials. R^2 values are given in Table 3, and they are very close to 1, which indicate the good nonlinear regression fitting and accurate predictions near T_g . Individually, the R^2 values of Pyrex and $\text{Se}_{90}\text{Te}_{10}$ are smaller, which is believed to be associated with the deviation of the collected data. As mentioned above, the accuracy of predicting some glass-forming liquids with high fragility is uncertain [16]; this analysis does not occur in this study.

Table 2. Obtained parameters of $7.9\text{Cs}_2\text{O}-23.2\text{CaO}-66.7\text{SiO}_2-1\text{Fe}_2\text{O}_3$ in the modified Eyring model and R^2 .

Parameters	$\log \eta_\infty$	m	T_g (K)	—	R^2
VFT	−4.89	35.92	1012.80	—	0.9996
AM	−2.42	32.75	1013.08	—	0.9994
MYEGA	−3.99	34.15	1012.95	—	0.9995
Parameters	C	D	H	β	—
Eyring	1.54	19,156.34	−4.74	−1185.31	0.9996

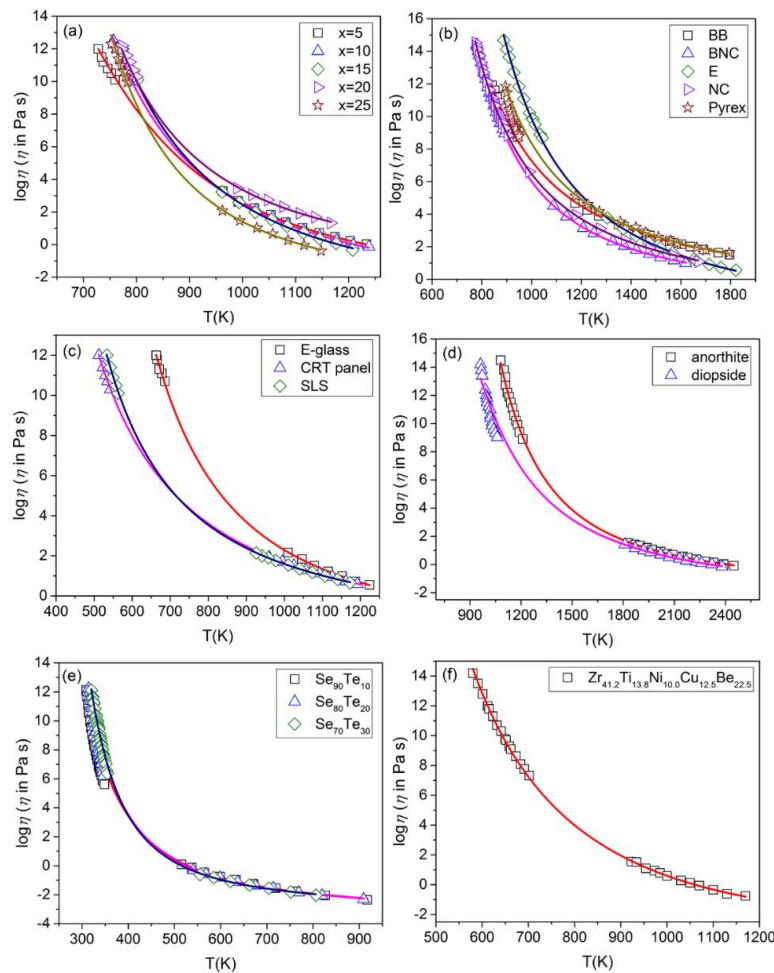


Figure 4. Comparison between predicted values and experimental viscosity values of different glasses: (a) $x\text{Na}_2\text{O}-10\text{CaO}-(89-x)\text{B}_2\text{O}_3-1\text{Fe}_2\text{O}_3$ ($x = 5, 10, 15, 20, 25$); (b) borosilicate melts; (c) silicate glass foam; (d) anorthite and diopside; (e) $\text{Se}_{90}\text{Te}_{10}$, $\text{Se}_{80}\text{Te}_{20}$ and $\text{Se}_{70}\text{Te}_{30}$ glass-forming system; (f) metallic glass- $\text{Zr}_{41.2}\text{Ti}_{13.8}\text{Ni}_{10.0}\text{Cu}_{12.5}\text{Be}_{22.5}$.

Table 3. R^2 of the predictions.

	Species	R^2		Species	R^2		Species	R^2
Figure 4a	x = 5	0.9996	Figure 4b	BB	0.9986	Figure 4c	E-glass	0.9998
	x = 10	0.9979		BNC	0.9999		CRT	0.9999
	x = 15	0.9996		E	0.9996		SLS	0.9999
	x = 20	0.9985		NC	0.9999	Figure 4d	anorthite	0.9993
	x = 25	0.9991		Pyrex	0.9674		diopside	0.9910
Figure 4e	Se ₈₀ Te ₂₀	0.9814	Figure 4f	metallic	0.9996			
	Se ₇₀ Te ₃₀	0.9976						
	Se ₉₀ Te ₁₀	0.9647						

4. Summary

In this work, a temperature-dependent viscosity model with a new mathematical expression was developed based on the Eyring pressure equation of viscosity and basic thermodynamic features of glass-forming liquids. The parameters of the equation were obtained from employing the high-temperature viscosity and T_g data in the state-of-the-art with the nonlinear regression analysis. Then the viscosity of the low-temperature region was accurately predicted, which verified the reliability of the modified Eyring model. It was found that the viscosity values simulated by using both high-temperature and low-temperature viscosity data show a higher accuracy than those of only using high-temperature viscosity data.

Furthermore, with recently developed artificial intelligence and machine learning techniques, the efficiency and accuracy of modeling are expected to be much higher. Along with more data available in the future, the equation may facilitate an improvement in the properties and functionalities of novel glasses.

Author Contributions: Conceptualization, C.C.; methodology, C.C. and L.S.; software, J.Y. and Y.D.; validation, C.C., Y.D. and Y.J.; formal analysis, C.C.; investigation, C.C.; resources, H.Z.; data curation, C.C. and G.C.; writing—original draft preparation, C.C.; writing—review and editing, H.Z., L.S., Q.Z. and G.C.; visualization, G.C.; supervision, Q.Z. and H.Z.; project administration, H.Z. and Q.Z.; funding acquisition, H.Z. and Q.Z. All authors have read and agreed to the published version of the manuscript.

Funding: H.Z. thanks the National Natural Science Foundation of China (NSFC51572082, 51872092), and Nanjing Glass Fiber Research and Design Institute, Sinoma Science and Technology Co., Ltd. for support.

Acknowledgments: We would like to thank Changjun Peng (East China University of Science and Technology, Shanghai 200237) for helpful discussions.

Conflicts of Interest: The authors declare no conflicts of interest.

References

1. Martendal, C.P.; de Oliveira, A.P.N. Glass viscosity at crystallization temperature: An approach. *J. Therm. Anal. Calorim.* **2017**, *130*, 1903–1912. [\[CrossRef\]](#)
2. Zheng, Q.J.; Mauro, J.C. Viscosity of glass-forming systems. *J. Am. Ceram. Soc.* **2017**, *100*, 6–25. [\[CrossRef\]](#)
3. Wang, X.C.; Chen, J.W.; Yu, X.M.; Fan, Y.; Duan, Z.K.; Jiang, Y.W.; Yang, F.Q.; Zhou, Y.X.; Yang, T.Q. Temperature-dependent dielectric response of antiferroelectric (Pb_{0.97}La_{0.02})(Zr_{0.50}Sn_{0.40}Ti_{0.10})O-3 ceramic. *J. Mater. Sci. Mater. Electron.* **2018**, *29*, 5634–5637. [\[CrossRef\]](#)
4. Ji, X.; Zeng, H.; Li, X.; Ye, F.; Chen, J.; Chen, G.; Mauro, J. High Glass Transition Temperature Barium Silicophosphate Glasses Designed with Topological Constraint Theory. *J. Am. Ceram. Soc.* **2016**, *99*, 1255–1258. [\[CrossRef\]](#)
5. Wang, K.; Zhou, Y.F.; Xu, W.T.; Xiang, M.; Li, X.Q.; Wang, Z.G. Reactive hot pressing of SiC-ZrC composites at low temperature. *J. Eur. Ceram. Soc.* **2017**, *37*, 849–854. [\[CrossRef\]](#)
6. Hrma, P. Arrhenius model for high-temperature glass-viscosity with a constant pre-exponential factor. *J. Non-Cryst. Solids* **2008**, *354*, 1962–1968. [\[CrossRef\]](#)

7. Le Losq, C.; Neuville, D.R. Molecular structure, configurational entropy and viscosity of silicate melts: Link through the Adam and Gibbs theory of viscous flow. *J. Non-Cryst. Solids* **2017**, *463*, 175–188. [[CrossRef](#)]
8. Xuan, W.; Wang, H.; Xia, D. Deep structure analysis on coal slags with increasing silicon content and correlation with melt viscosity. *Fuel* **2019**, *242*, 362–367. [[CrossRef](#)]
9. Xuan, W.; Wang, H.; Xia, D. Depolymerization mechanism of CaO on network structure of synthetic coal slags. *Fuel Process. Technol.* **2019**, *187*, 21–27. [[CrossRef](#)]
10. Wang, K.; Lu, Q.H.; Yi, Y.Y.; Yi, J.L.; Niu, B.; Jiang, Z.X.; Ma, J.J. Effects of Welding Heat Input on Microstructure and Electrochemical Behavior of Flux-Cored Arc-Welded Q690 HSLA Steel. *Adv. Mater. Sci. Eng.* **2018**. [[CrossRef](#)]
11. Zheng, Q.; Mauro, J.C.; Yue, Y. Reconciling calorimetric and kinetic fragilities of glass-forming liquids. *J. Non-Cryst. Solids* **2017**, *456*, 95–100. [[CrossRef](#)]
12. Fulcher, G.S. Analysis of recent measurements of the viscosity of glasses. *J. Am. Ceram. Soc.* **2010**, *8*, 339–355. [[CrossRef](#)]
13. Scherer, G.W. Editorial Comments on a Paper by Gordon S. Fulcher. *J. Am. Ceram. Soc.* **2010**, *75*, 1060–1062. [[CrossRef](#)]
14. Adam, G.; Gibbs, J.H. On the Temperature Dependence of Cooperative Relaxation Properties in Glass-Forming Liquids. *J. Chem. Phys.* **1965**, *43*, 139–146. [[CrossRef](#)]
15. Avramov, I.; Milchev, A. Effect of disorder on diffusion and viscosity in condensed systems. *J. Non-Cryst. Solids* **1988**, *104*, 253–260. [[CrossRef](#)]
16. Mauro, J.C.; Yue, Y.Z.; Ellison, A.J.; Gupta, P.K.; Allan, D.C. Viscosity of glass-forming liquids. *Proc. Natl. Acad. Sci. USA* **2009**, *106*, 19780–19784. [[CrossRef](#)]
17. Hrma, P.; Kruger, A.A. High-temperature viscosity of many-component glass melts. *J. Non-Cryst. Solids* **2016**, *437*, 17–25. [[CrossRef](#)]
18. Martins, R.J.; de Cardoso, M.J.E.; Barcia, O.E. A New Model for Calculating the Viscosity of Pure Liquids at High Pressures. *Ind. Eng. Chem. Res.* **2003**, *42*, 3824–3830. [[CrossRef](#)]
19. Sun, H.B.; Wang, Y.F. Glass Forming Ability, Thermal Stability, and Magnetic Properties of FeCoNiBSi Alloys with Different B Contents. *Adv. Mater. Sci. Eng.* **2018**, *2018*, 4841025. [[CrossRef](#)]
20. Hrma, P. Glass viscosity as a function of temperature and composition: A model based on Adam–Gibbs equation. *J. Non-Cryst. Solids* **2008**, *354*, 3389–3399. [[CrossRef](#)]
21. Kincaid, J.F.; Eyring, H.; Stearn, A.E. The Theory of Absolute Reaction Rates and its Application to Viscosity and Diffusion in the Liquid State. *Chem. Rev.* **1941**, *28*, 301–365. [[CrossRef](#)]
22. Xuan, A.G.; Wu, Y.X.; Peng, C.J.; Ma, P.S. Correlation of the viscosity of pure liquids at high pressures based on an equation of state. *Fluid Phase Equilib.* **2006**, *240*, 15–21. [[CrossRef](#)]
23. He, M.G.; Zhu, C.Y.; Liu, X.Y. Estimating the viscosity of ionic liquid at high pressure using Eyring’s absolute rate theory. *Fluid Phase Equilib.* **2018**, *458*, 170–176. [[CrossRef](#)]
24. And, C.D.; Kiran, E. High-Pressure Viscosity and Density of Polymer Solutions at the Critical Polymer Concentration in Near-Critical and Supercritical Fluids. *Ind. Eng. Chem. Res.* **2002**, *41*, 6354–6362.
25. Yan, X.; Kiran, E. Miscibility, density and viscosity of polystyrene in n-hexane at high pressures. *Polymer* **1997**, *38*, 5185–5193.
26. Gaudio, P.D.; Behrens, H.; Deubener, J. Viscosity and glass transition temperature of hydrous float glass. *J. Non-Cryst. Solids* **2007**, *353*, 223–236. [[CrossRef](#)]
27. Eyring, H. Viscosity, Plasticity, and Diffusion as Examples of Absolute Reaction Rates. *J. Chem. Phys.* **2004**, *4*, 283–291. [[CrossRef](#)]
28. Ojovan, M.I. Viscous flow and the viscosity of melts and glasses. *Phys. Chem. Glasses-B* **2012**, *53*, 143–150.
29. Geerissen, H.; Schmidt, J.R.; Wolf, B.A. On the factors governing the pressure dependence of the viscosity of moderately concentrated polymer solutions. *J. Appl. Polym. Sci.* **1982**, *27*, 1277. [[CrossRef](#)]
30. Wolf, B.A.; Jend, R. Pressure and Temperature Dependence of the Viscosity of Polymer Solutions in the Region of Phase Separation. *Macromolecules* **1979**, *12*, 732–737. [[CrossRef](#)]
31. Tverjanovich, A.S. Temperature dependence of the viscosity of chalcogenide glass-forming melts. *Glass Phys. Chem.* **2003**, *29*, 532–536. [[CrossRef](#)]
32. Wang, Y.; Sakamaki, T.; Skinner, L.B.; Jing, Z.; Yu, T.; Kono, Y.; Park, C.; Shen, G.; Rivers, M.L.; Sutton, S.R. Atomistic insight into viscosity and density of silicate melts under pressure. *Nat. Commun.* **2014**, *5*, 3241. [[CrossRef](#)] [[PubMed](#)]

33. Chow, K.C.; Wong, S.; Kui, H.W. The specific volumes of Pd₄₀Ni₄₀P₂₀ in the liquid, glass, and crystallized states. *J. Appl. Phys.* **1993**, *74*, 5410–5414. [\[CrossRef\]](#)
34. Jabraoui, H.; Malki, M.; Hasnaoui, A.; Badawi, M.; Ouaskit, S.; Lebegue, S.; Vaills, Y. Thermodynamic and structural properties of binary calcium silicate glasses: Insights from molecular dynamics. *Phys. Chem. Chem. Phys.* **2017**, *19*, 19083–19093. [\[CrossRef\]](#) [\[PubMed\]](#)
35. Tischendorf, B.C.; Alam, T.M.; Cygan, R.T.; Otaigbe, J.U. The structure and properties of binary zinc phosphate glasses studied by molecular dynamics simulations. *J. Non-Cryst. Solids* **2003**, *316*, 261–272. [\[CrossRef\]](#)
36. Deng, L.; Du, J. Effects of system size and cooling rate on the structure and properties of sodium borosilicate glasses from molecular dynamics simulations. *J. Chem. Phys.* **2018**, *148*, 024504. [\[CrossRef\]](#)
37. Ediger, M.D.; Angell, C.A.; Nagel, S.R. Supercooled Liquids and Glasses. *J. Phys. Chem.* **1996**, *100*, 13200–13212. [\[CrossRef\]](#)
38. Smedskjaer, M.M.; Mauro, J.C.; Yue, Y. Ionic diffusion and the topological origin of fragility in silicate glasses. *J. Chem. Phys.* **2009**, *131*, 244514. [\[CrossRef\]](#)
39. Laughlin, W.T.; Uhlmann, D.R. Viscous flow in simple organic liquids. *J. Phys. Chem.* **1972**, *76*, 2317–2325. [\[CrossRef\]](#)
40. Angell, C.A. Spectroscopy simulation and scattering, and the medium range order problem in glass. *J. Non-Cryst. Solids* **1985**, *73*, 1–17. [\[CrossRef\]](#)
41. Zheng, Q.J.; Mauro, J.C.; Smedskjaer, M.M.; Youngman, R.E.; Potuzak, M.; Yue, Y.Z. Glass-forming ability of soda lime borate liquids. *J. Non-Cryst. Solids* **2012**, *358*, 658–665. [\[CrossRef\]](#)
42. Petersen, R.R.; Konig, J.; Yue, Y.Z. The viscosity window of the silicate glass foam production. *J. Non-Cryst. Solids* **2017**, *456*, 49–54. [\[CrossRef\]](#)
43. Sipp, A.; Neuville, D.R.; Richet, P. Viscosity, configurational entropy and relaxation kinetics of borosilicate melts. *J. Non-Cryst. Solids* **1997**, *211*, 281–293. [\[CrossRef\]](#)
44. Košťál, P.; Málek, J. Viscosity of Se–Te glass-forming system. *Pure Appl. Chem.* **2015**, *87*, 239–247. [\[CrossRef\]](#)
45. Suzuki, H.; Kanazawa, I. Viscosities of the Zr-based bulk metallic glass-forming liquids. *Intermetallics* **2010**, *18*, 1809–1812. [\[CrossRef\]](#)



© 2020 by the authors. Licensee MDPI, Basel, Switzerland. This article is an open access article distributed under the terms and conditions of the Creative Commons Attribution (CC BY) license (<http://creativecommons.org/licenses/by/4.0/>).